Monitoring the Distribution of Covalently Tethered Sugar Moieties in Sol−Gel-Based Silica Monoliths with Fluorescence Anisotropy: Implications for Entrapped Enzyme Activity

Xihua Sui,[†] Tsai-Yin Lin,[†,‡] Dina Tleugabulova,[†] Yang Chen,[†] Michael A. Brook,[†] and John D. Brennan*[,†]

Department of Chemistry, McMaster University, Hamilton, ON, L8S 4M1 Canada, and Department of Biomedical Engineering and Environmental Sciences, National Tsing Hua University, Hsinchu 30013, Taiwan, ROC

Received August 17, 2005. Revised Manuscript Received December 13, 2005

Biocompatible silica derived from diglycerylsilane (DGS) and the sugar modified silane *N*-(3-triethoxysilylpropyl)gluconamide (GLS) has been shown to have great utility for the entrapment of a number of delicate proteins. To further understand the nature of the DGS/GLS composite material, it is important to characterize the local microenvironment and properties of the silica surface within the DGS/GLS monoliths. In this work, we have monitored both the steady-state and time-resolved anisotropy of the fluorescent probe rhodamine 6G (R6G) to determine the distribution of GLS within DGS/GLS-derived materials where varying levels of GLS were added either to the sol or to previously formed DGS-based gels. The data suggest that the addition of GLS to an evolving sol results in preferential coating of silica nanoparticles, which remain present in the gelled material and slowly associate with the continuous polymer network. The preferential presence of GLS on the surface of free particles results in inefficient coating of the monolithic material with the sugarsilane and causes most of the added R6G to associate with the silica skeleton. On the other hand, the addition of GLS to a preformed monolith results in preferential modification of the monolithic silica surface and a much increased level of free dye. A significant amount of R6G-bound nanoparticles remain within these materials over an extended time, suggesting that the nanoparticles do not associate with the GLS-modified silica monolith. The activity of the enzyme horseradish peroxidase was evaluated in DGS derived materials that had GLS added to either the sol or the monolith, and it was determined that optimal activity was obtained in cases where GLS was added to the sol. These results highlight the importance of controlling the time of addition of organosilane additives to evolving sols and suggest that this factor might provide a means to control the properties of the resulting nanocomposite material.

Introduction

In recent years, a number of sol−gel-derived materials have been designed with the purpose of making the matrix more compatible with entrapped biological molecules. For example, new biocompatible silane precursors and processing methods have recently been reported that are based on glycerated silanes,[1,2] sodium silicate,[3] or aqueous processing methods that involve removal of alcohol byproducts by evaporation before the addition of proteins.[4] Other approaches to improve protein stability, including the use of protein-stabilizing additives such as organosilanes,[5−7] polymers,[8−12] or sugars and amino acids (osmolytes)[13,14], have also been reported.

Recently, our group reported two advances in the development of sol−gel-processed materials: (1) the development of new sol−gel precursors, such as diglycerylsilane (DGS), that release protein-stabilizing compounds upon hydrolysis,[1,15] and (2) the preparation of silica precursors bearing covalently bound sugars, such as gluconamidylsilane (GLS),[16]

* To whom correspondence should be addressed. Tel.: (905) 525-9140 (ext. 27033). Fax: (905) 527-9950. E-mail: brennanj@mcmaster.ca. Internet: http://www.chemistry.mcmaster.ca/faculty/brennan.

[†] McMaster University.

[‡] National Tsing Hua University.

(1) (a) Brook, M. A.; Chen, Y.; Guo, K.; Zhang, Z.; Jin, W.; Deisingh, A.; Brennan, J. D. *J. Sol−Gel Sci. Technol.* **2004**, *31*, 343. (b) Brook, M. A.; Chen, Y.; Guo, K.; Zhang, Z.; Brennan, J. D. *J. Mater. Chem.* **2004**, *14*, 1469.
(2) Gill, I.; Ballesteros, A. *J. Am. Chem. Soc.* **1998**, *120*, 8587.
(3) Bhatia, R. B.; Brinker, C. J.; Gupta, A. K.; Singh, A. K. *Chem. Mater.* **2000**, *12*, 2434.
(4) Ferrer, M. L.; del Monte, F.; Levy, D. *Chem. Mater.* **2002**, *14*, 3619.
(5) Reetz, M. T.; Zonta, A.; Simpelkamp, J.; Konen, W. *Chem. Commun.* **1996**, 1397.
(6) Reetz, M. T.; Zonta, A.; Simpelkamp, J. *Angew. Chem., Int. Ed. Engl.* **1995**, *34*, 301.
(7) Kuncova, G.; Guglielmi, M.; Dubina, P.; Safar, B. *Collect. Czech. Chem. Commun.* **1995**, *60*, 1573.
(8) Altstein, M.; Segev, G.; Aharonson, N.; Ben-Aziz, O.; Turniansky, A.; Avnir, D. *J. Agric. Food Chem.* **1998**, *46*, 3318.
(9) Wang, B. Q.; Li, B.; Deng, Q.; Dong, S. J. *Anal. Chem.* **1998**, *70*, 3170.
(10) Wang, B. Q.; Dong, S. J. *Talanta* **2000**, *51*, 565.
(11) Zhang, J. Z.; Li, B.; Wang, Z.-X.; Cheng, G. J.; Dong, S. J. *Anal. Chim. Acta* **1999**, *388*, 71.
(12) (a) Chen, Q. Kenausis, G. L.; Heller, A. *J. Am. Chem. Soc.* **1998**, *120*, 4582. (b) Heller, J.; Heller, A. *J. Am. Chem. Soc.* **1998**, *120*, 4586.
(13) Eggers, D. K.; Valentine, J. S. *J. Mol. Biol.* **2001**, *314*, 911.
(14) Brennan, J. D.; Benjamin, D.; Dibattista, E.; Gulcev. M. D. *Chem. Mater.* **2003**, *15*, 737.
(15) Besanger, T. R.; Chen, Y.; Deisingh, A. K.; Hodgson, R.; Jin, W.; Stanislas, M.; Brook, M. A.; Brennan, J. D. *Anal. Chem.* **2003**, *75*, 2382.

10.1021/cm051853z CCC: $33.50
Published on Web 02/01/2006

which result in the formation of sugar-modified silica materials. Together, these compounds have been shown to produce low-shrinkage materials that are amenable to entrapment of a number of delicate proteins, including urease, Factor Xa, Src Kinase, and luciferase, none of which remain active upon entrapment in silica materials derived from conventional alkoxysilanes.

Although sugar-modified silica materials have been demonstrated to be suitable hosts for entrapped proteins[16,17] and have been shown to be less susceptible to shrinkage and cracking than unmodified materials,[18] little work has been done regarding the characterization of the pore environment within such materials. It is known that the presence of organic moieties within sol−gel materials has a great impact on the microenvironment and properties of silica materials.[19] For this reason, the focus of this work is to explore (1) the degree of silica surface modification by sugarsilanes using different modification protocols; (2) the distribution of sugarsilanes between different microenvironments; (3) the influence of the presence of sugar moieties on the drying behavior of DGS/GLS based silica monoliths; and (4) the effects of the presence, timing of addition, and distribution of the sugarsilane on the activity of the entrapped enzyme horseradish peroxidase (HRP).

The two modification protocols used in the present work are: (1) the mixing of hydrolyzed DGS and GLS monomers at the sol stage followed by gelation; and (2) the modification of preformed DGS derived monoliths by the addition of GLS. The co-condensation of hydrolyzed DGS and GLS monomers is expected to result in the formation of GLS-coated silica colloids prior to monolith formation, whereas the addition of GLS to a preformed monolith should avoid the possibility of colloidal modification prior to monolith formation. Comparison of these methods allows for a determination of the nature of the resulting silica material as a function of both time of addition and concentration of the modifier.

For the examination of the surface properties of the monolithic silica, we monitored the steady-state and time-resolved fluorescence anisotropy of rhodamine 6G (R6G). This probe has been previously utilized to examine the growth[20−26] and degree of surface modification[27−30] of silica nanoparticles. Assessment of surface modification relies on measuring the ratio of rapidly rotating R6G (picosecond correlation time), corresponding to free dye in solution, to slowly rotating (nanosecond correlation time) or nonrotating (which results in a residual anisotropy value) dye, which is bound to small and large silica particles, respectively. For unmodified silica, the proportion of bound dye is generally in the range of 95−99%.[27−30] Addition of surface modifiers, such as polymers, organosilanes, or peptides, results in a blockage of the anionic silica surface, so that less of the cationic probe adsorbs. This is observed as a decrease in the proportion of bound dye. By measuring the ratio of bound dye in modified and unmodified samples, it is possible to assess the extent of surface modification by the modifier.[27,29]

Herein, we examine the anisotropy behavior of R6G in monolithic silica containing varying levels of GLS that are added to either the sol or the preformed monolith. Studies of R6G anisotropy within polymer[31] and organosilane-modified[32] silica derived from tetramethoxysilane (TMOS) have been previously reported by Bright and co-workers. However, the presence of high levels of methanol as a byproduct of TMOS hydrolysis significantly altered the solubility of the dye in the solvent phase and, hence, the partitioning of the dye between bound and free states. The present study represents the first time that the time-resolved fluorescence anisotropy (TRFA) approach has been applied to silica monoliths that do not liberate simple alcohols, as well as the first time that the "nanoparticle metrology" model has been used to interpret the R6G TRFA data in terms of surface modification of a monolithic material. We show that the method can provide unique information about the formation and surface modification of sol−gel-derived monolithic materials. In addition, this tool permitted us to demonstrate that the timing of GLS addition is important in controlling the properties of the resulting material. Finally, the activity of the enzyme horseradish peroxidase was evaluated in DGS materials that had had GLS added to either the sol or the monolith to determine whether the timing of addition, and hence the distribution of GLS moieties, had an impact on the biological compatibility of the material.

Experimental Section

Chemicals. Diglycerylsilane (DGS, MW 208) and *N*-(3-triethoxysilylpropyl) gluconamide (GLS, MW 399) were synthesized as described elsewhere.[1,28] Rhodamine 6G (R6G) and was purchased from Sigma (St. Louis, MO). Horseradish peroxidase (E.C. 1.11.1.7), guaiacol, and hydrogen peroxide were obtained from Aldrich (Oakville, ON, Canada). All water was distilled and deionized on a Milli-Q Synthesis A10 water purification system. All reagents were used without further purification.

Sample Preparation. The sol−gel monoliths were prepared using different protocols (denoted A, B and C) for incorporation of both GLS and R6G, as described below.

Sample A. These samples had both GLS and R6G added at the sol stage. For sample A1, sols were prepared by a brief and vigorous

(16) (a) Cruz-Aguado, J. A.; Chen, Y.; Zhang, Z.; Elowe, N.; Brook, M. A.; Brennan, J. D. *J. Am. Chem. Soc.* **2004**, *126*, 6878. (b) Cruz-Aguado, J. A.; Chen, Y.; Brook, M. A.; Brennan, J. D. *Anal. Chem.* **2004**, *76*, 4182.
(17) Sui, X.; Cruz-Aguado, J. A.; Chen, D. Y.; Zhang, Z.; Brook, M. A.; Brennan, J. D. *Chem. Mater.* **2005**, *17*, 1174.
(18) Chen, Y.; Zhang, Z.; Sui, X.; Brennan, J. D.; Brook, M. A. *J. Mater. Chem.* **2005**, *15*, 3132.
(19) Castelvetro, V.; De Vita, C. *Adv. Colloid Interface Sci.* **2004**, *108−109*, 167.
(20) Geddes, C. D.; Birch, D. J. S. *J. Non-Cryst. Solids* **2000**, *270*, 191.
(21) Birch, D. J. S.; Geddes, C. D. *Phys. Rev. E.* **2000**, *62*, 2977.
(22) Geddes, C. D.; Karolin, J.; Birch, D. J. S. *J. Fluoresc.* **2002**, *12*, 113.
(23) Geddes, C. D.; Karolin, J.; Birch, D. J. S. *J. Fluoresc.* **2002**, *12*, 135.
(24) Geddes, C. D. *J. Fluoresc.* **2002**, *12*, 343.
(25) Tleugabulova, D.; Zhang, Z.; Brennan, J. D. *J. Phys. Chem. B* **2003**, *107*, 10127.
(26) Tleugabulova, D.; Duft, A. M.; Zhang, Z.; Chen, Y.; Brook, M. A.; Brennan, J. D. *Langmuir* **2004**, *20*, 5924.
(27) Tleugabulova, D.; Duft, A. M.; Brook, M. A.; Brennan, J. D. *Langmuir* **2004**, *20*, 101.
(28) Tleugabulova, D.; Zhang, Z.; Chen, Y.; Brook, M. A.; Brennan, J. D. *Langmuir* **2004**, *20*, 848.
(29) Sui, J.; Tleugabulova, D.; Brennan J. D. *Langmuir* **2005**, *21*, 4996.
(30) Tleugabulova, D.; Sui, J.; Ayers, P.; Brennan, J. D. *J. Phys. Chem. B* **2005**, *109*, 7850.
(31) Baker, G.A.; Jordan,. J. D.; Bright, F. V. *J. Sol−Gel Sci. Technol.* **1998**, *11*, 43.
(32) Baker, G. A.; Pandey, S.; Maziarz, E. P., III; Bright, F. V. *J. Sol−Gel Sci. Technol.* **1999**, *15*, 37.

dissolution of 0.25 g of DGS in 1 mL of water at room temperature, followed by immediate dilution (1/1, v/v) of the dissolved DGS with 25 mM Tris-HCl buffer, pH 8.3, containing R6G and GLS to a volume of 2 mL. The GLS stock solutions were prepared immediately before use by dissolving GLS (0.17−0.3 g) in 0.5 mL of Tris-HCl buffer. After being mixed, the DGS/GLS sols (pH 7.5) were immediately poured into polymethacrylate fluorimeter cuvettes (transmittance curve C) from Sigma. The DGS monolith was formed in 2 min after DGS dissolution and contained 0.6 M DGS, 3.6 wt % SiO_2, and 1 μM R6G. The DGS/GLS monoliths were formed in 2−4 min after sol preparation and contained 0.6 M DGS, 25 or 40 mol % GLS, 4.8−5.8 wt % SiO_2, and 1 μM R6G.

In a second procedure (A2) designed to mimic the method used for protein entrapment,[16] the DGS stock solution was obtained by dissolving 0.4 g of crushed DGS powder in 1 mL of chilled water and then sonicating for 1 h in chilled water. The transparent DGS solution was then filtered using a 0.22-μm Acrodisc syringe filter (Pall Corp., Ann Arbor, MI) to remove large particulates. The GLS stock solution was prepared by dissolving varying levels of GLS in 5 mL of 25 mM Tris-HCl, pH 7.4. The plain DGS sols were prepared by mixing 1 mL of the DGS-derived sol with 1 mL of Tris-HCl buffer or GLS stock solution containing R6G. The DGS/GLS monoliths were formed in 2−4 min after sol preparation and contained 0.6 M DGS, 4.8−5.8 wt % SiO_2, 0−20 mol % GLS, and 1 μM R6G. The monoliths were aged at 4 °C in air prior to fluorescence analysis. We estimate that the amounts of glycerol and ethanol as byproducts of DGS and GLS hydrolyses do not exceed 11.5% and 3.3% (v/v), respectively.

Sample B. These samples had GLS added to the sol and R6G added to the monolith to probe only accessible regions of the sample. In this case, DGS and DGS/GLS monoliths were prepared as described above (sample A2) but with no R6G present. After gelation, the preformed DGS/GLS monolith was equilibrated for 24 h with 2 mL of a solution containing 1 μM R6G. The solution above the monolith was then removed, and the samples were aged in air for a specified period of time prior to sample analysis. Note that, after 24 h, the R6G dye was observed to be homogeneously distributed through the gel block.

Sample C. These samples had both GLS and R6G added to preformed DGS monoliths. DGS monoliths were prepared as described above (sample A2) and allowed to gel. After 24 h, the monoliths were incubated with 2 mL of a GLS stock solution (with concentrations identical to those used for the formation of monoliths) for 24 h at room temperature. After the equilibration with GLS, the top solution was removed, and the monoliths were equilibrated with 1 μM R6G aqueous solution (2 mL) for an additional 24 h. The top liquid was then removed, and the samples were aged in air for a specific period of time and then subjected to fluorescence analysis.

Shrinkage Measurements. Shrinkage measurements were performed on samples that had been aged in air for 47 days, after which time there were no observable changes in sample mass owing to drying. Samples were prepared as blocks with initial dimensions of 1 cm × 1 cm × 2 cm. The volume of the materials after aging was determined by measurement of the dimensions of the shrunken blocks, and shrinkage values are reported relative to the original volume of the block.

Steady-State Fluorescence Anisotropy (SSFA). Single-point fluorescence anisotropy measurements for R6G were performed using an SLM 8100 spectrofluorimeter (Spectronic Instruments, Rochester, NY) with $\lambda_{ex} = 495$ nm and $\lambda_{em} = 551$ nm, as described elsewhere.[25] Appropriate blanks were subtracted from each of the intensity values (I_{VV}, I_{VH}, I_{HV}, I_{HH}) used to calculate the anisotropy values, and all data were corrected for the instrumental G factor to account for any polarization bias in the monochromators. Each anisotropy value reported represents the average of three independent measurements (five replicates per sample) performed on three different samples.

Time-Resolved Fluorescence Anisotropy (TRFA). Time-resolved fluorescence intensity and anisotropy decay data were acquired in the time domain using an IBH 5000U time-correlated single-photon-counting fluorimeter (Edinburgh, U.K.) with a 495-nm NanoLED source run at 1 MHz and an IBH model TBX-04 photon-counting PMT detector. A detailed description of the instrumentation and experimental procedures has been previously reported.[25] The fluorescence decays collected by exciting samples with vertically polarized light were used to generate the sum [$S(t)$] and difference [$D(t)$] functions, which were used to construct the anisotropy decay [$r(t)$] as

$$r(t) = \frac{D(t)}{S(t)} = \frac{I_{VV}(t) - GI_{VH}(t)}{I_{VV}(t) + 2GI_{VH}(t)} \quad (1)$$

where G is the experimentally measured polarization bias of the monochromator/PMT.

The anisotropy decay was fit to the equation

$$r(t) = f_1 r_0^{exp} \exp(-t/\phi_1) + f_2 r_0^{exp} \exp(-t/\phi_2) + g r_0^{exp} \quad (2)$$

where ϕ_1 and ϕ_2 are the picosecond and nanosecond rotational correlation times, respectively; f_1 and f_2 are the fractional contributions of ϕ_1 and ϕ_2, respectively, to $r(t)$; r_0^{exp} is the experimental initial anisotropy at $t = 0$, which corresponds to the anisotropy after internal conversion and vibrational relaxation, prior to probe rotation; and g is the fractional contribution from the nondecaying component, calculated as $g = r_\infty / r_0^{exp}$, where r_∞ is the residual anisotropy and $f_1 + f_2 + g = 1$.[30] The fitted r_0^{exp} value should nearly correspond to steady-state anisotropy of R6G in a glassy frozen solvent, $r_0^{exp} = r_0^{R6G} = 0.38$.[33] The fits were considered acceptable if the reduced chi-squared value, χ_R^2, was close to 1.0 and the residuals show a random pattern.

Entrapment of HRP. All samples were prepared by method A2 (DGS and DGS/GLS) or method C (addition of GLS to a preformed DGS monolith). DGS monoliths were prepared by dispensing 30 μL of a HRP/Tris-HCl solution (25 mM Tris, pH 7.0) in the bottoms of the wells in a 96-well microtiter plate. The same volume of DGS sol (0.4 g/mL) was then added to each of the samples within the microwells and rapidly mixed using a microtiter plate shaker, giving a final sample volume of 60 μL. The contents of the wells gelled within 5 min, yielding homogeneous monoliths with a final HRP concentration of 0.2 μg/mL. Buffer (30 μL) with different amounts of GLS (0−158 mg/ml) was added onto the top of the DGS gels to prepare GLS-modified DGS monoliths. Preparation of DGS/GLS was done by adding different amounts of GLS to the HRP/Tris-HCl solution and then mixing with an equal portion of DGS sol. Samples were typically tested for HRP activity 1 day after gelation.

HRP Activity Assay. All gels were first washed with 0.5 mL of buffer solution to remove excess additives such as glycerol or unbound GLS before the activity assay commenced. HRP activity was assayed in 96 well plates using the guiacol test method.[34] Briefly, 30 μL of 4.8 mM guiacol in water (pH 7.0) was added into each well and equilibrated for 30 min, which was shown to be

(33) Narang, U.; Wang, R.; Prasad, P. N.; Bright, F. V. *J. Phys. Chem.* **1994**, *98*, 17.
(34) (a) Savenkova, M. I. J.; Kuo, M.; de Montellano P. R. O. *Biochemistry* **1998**, *37*, 10828. (b) Hayashi, T.; Hitomi, Y.; Ando, T.; Mizutani, T.; Hisaeda, Y.; Kitagawa, S.; Ogoshi, H. *J. Am. Chem. Soc.* **1999**, *121*, 7747.

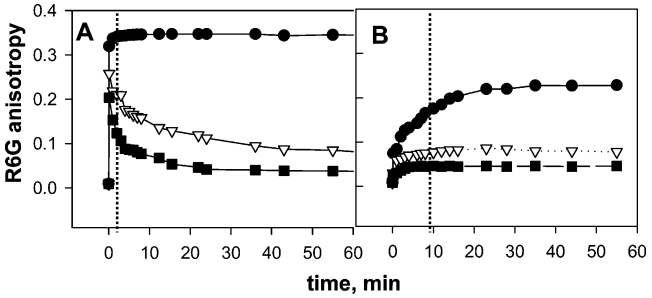

Figure 1. SSFA of R6G in (●) DGS and (▽, ■) DGS/GLS sols as a function of time. Error, ±0.001; solvent, 25 mM Tris-HCl, pH 8.3; final pH, 7.5; DGS concentration, 0.6 M; GLS concentration, (▽) 25 and (■) 40 mol %; total SiO_2 concentration, (●) 3.6, (▽) 4.8, and (■) 5.8 wt %. Initial zero time corresponds to DGS dissolution at room temperature (sample A1, panel A) or after 1 h of sonication of DGS in chilled water (sample A2, panel B). Initial anisotropy value corresponds to R6G anisotropy in buffer in the absence of DGS. Measurements were performed at 295 K, λ_{ex} = 495 nm, and λ_{em} = 551 nm. Dotted vertical line indicates the gelation point.

sufficient to reach equilibrium. At this point, 20 μL of 0.97 mM hydrogen peroxide in 25 mM Tris-HCl buffer was added to the well to achieve final concentrations of 2.9 mM guiacol and 0.39 mM hydrogen peroxide. Absorbance was monitored at 470 nm over a period of 30 min using a TECAN Safire absorbance/fluorescence plate reader, and activity was determined from the initial slope of the response curve and normalized to the activity of HRP in unmodified DGS materials.

Results and Discussion

SSFA Analysis of DGS/GLS Sols. Previous studies of DGS-derived sols and gels[26] have shown that the precursor undergoes rapid hydrolysis and condensation to form primary and secondary particles, followed by slower, pH-dependent growth and aggregation of the colloidal particles to eventually form a continuous gel network. Unlike systems derived from TEOS or sodium silicate, the presence of high levels of glycerol as a byproduct of DGS hydrolysis leads to stabilization of the initially formed particles over long periods of time.[26] As a starting point for the investigation of the DGS/GLS system, we first investigated the steady-state anisotropy of R6G in DGS-derived sols and gels for which two different methods had been used to prepare the sols. In unfiltered DGS sols (sample A1), the R6G anisotropy spiked immediately after DGS dissolution (Figure 1a), reaching a value of r = 0.341 at the gelation point (t_g = 2 min), which indicates the formation of a highly polymerized silica surface. Under similar conditions that promote fast silica particle growth and polymerization, the R6G anisotropy in an aqueous sodium silicate sol is also high (r = 0.35)[27] and close to the limiting anisotropy, r_0 = 0.38[33] This indicates significant restriction of the rotational diffusion of R6G when bound to either the immobile silica network or silica nanoparticles of radius R > 2.5 nm.[27] After the gelation of DGS, the R6G anisotropy gradually increased to r = 0.347, as a result of further silica polymerization. We note that the anisotropy values obtained for our materials are significantly higher that those reported by Bright et al. for R6G dispersed in TMOS-derived materials.[31,32] This is due to the presence of methanol in the latter materials, which causes a significant fraction of the R6G to be located in solvent-filled pores rather than being associated with the silica surface. R6G is far less soluble in the glycerol/water pore solvent in our materials[25] and, thus, is more highly associated with the silica surface.

The DGS sol used for protein entrapment was prepared by 1 h of sonication in chilled water to prevent fast silica particle growth prior to complete DGS dissolution and was filtered to remove any large particles to slow the rate of gelation. SSFA analysis of this sol showed much lower initial and plateau anisotropies for R6G, even after gelation of the sol (Figure 1b). The lower anisotropy values and slower gelation are consistent with the DGS sol containing mostly small silica nanoparticles. Importantly, the lower plateau anisotropy value clearly indicates that R6G is not fully associated with the surface of the monolithic silica skeleton in such materials. This must be due either to a higher fraction of free R6G or to a higher proportion of R6G bound to small silica nanoparticles that are still able to rotate within the monolithic silica network. Because the solubility of R6G would not be expected to be different within the pore solvent of either material, it is most likely that the lower anisotropy is due to the presence of small silica nanoparticles in the filtered material. This interpretation is corroborated by TRFA data (see below).

To monitor the effect of GLS on the early stages of silica condensation, the DGS/GLS sols were prepared by immediate dissolution and mixing of the two components, followed by monitoring of the steady-state fluorescence anisotropy (SSFA) of the added R6G. For sol studies, high amounts of GLS were used (25 or 40 mol %), as these levels provided significant alterations in the SSFA data, making data interpretation more straightforward. Note that solutions consisting of R6G and GLS showed only a single picosecond-scale anisotropy decay time, indicating that there was no direct interaction between these species, consistent with the findings obtained for R6G analysis of GLS-coated silica nanoparticles.[28] Thus, all changes in R6G anisotropy can be ascribed to alterations in R6G−silica interactions.

In the presence of GLS, the R6G anisotropy of unfiltered DGS sols spiked at the gelation point, but to a value lower than that measured in the plain DGS sol (Figure 1a). The spike indicates the formation of silica nanoparticles to which R6G can bind, providing evidence that the rate of silica condensation remains high even in the presence of GLS. Thus, the formation of silica nanoparticles is the earliest event of the sol−gel reaction in DGS/GLS sols. The lower anisotropy value at the gelation point relative to that of unmodified DGS sols and the decrease in anisotropy beyond the gelation point reflect the gain in rotational mobility of R6G as a result of its partial displacement by GLS molecules from the polymerized silica particles/monolith to the water-filled pores.

Beyond the gelation point, there was a continuous, concentration-dependent decrease in the R6G anisotropy for the next 50 min. This indicates the further displacement of silica-bound R6G molecules by GLS molecules. At GLS levels of 25 and 40 mol %, the lowest plateau values reached at 40 min were r = 0.08 and r = 0.04, respectively. This clearly demonstrates that the GLS modification of the silica surface continues after the formation of the silica monolith, which can be interpreted to arise from the presence of a large

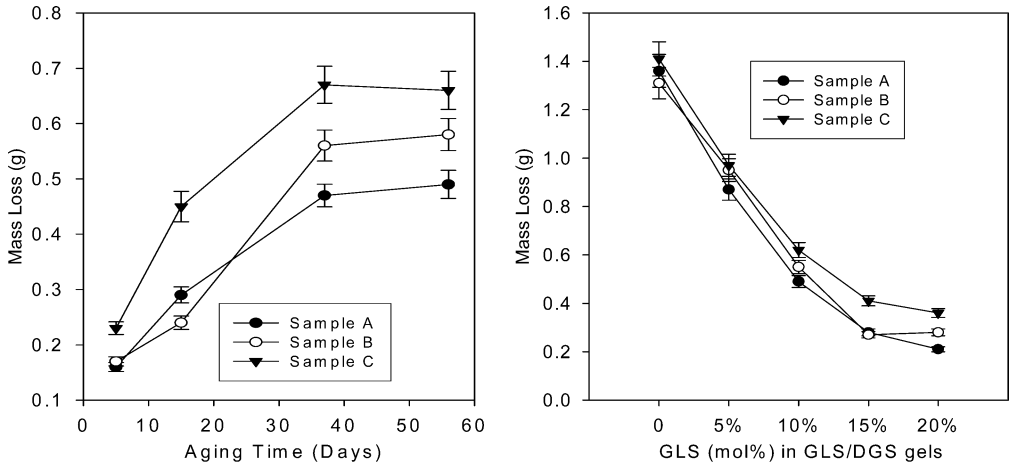

Figure 2. (a) Loss of mass for monoliths containing 10 mol % GLS prepared by routes A−C over 58 days of aging in air. (B) Loss of mass on day 58 for monoliths prepared by routes A−C as a function of the amount of added GLS.

portion of GLS monomers that are physically entrapped in the silica pores immediately after monolith formation. These GLS molecules would lead to the localization of sugar moieties at the silica/water interfaces rather than in the silica core of the sol−gel network.

Coating filtered DGS sols with GLS (Figure 1b) did not lead to the presence of spikes in the anisotropy curves, consistent with slower particle formation in this system. In this case, it is likely that the GLS initially binds to the surface of slowly growing silica nanoparticles, preventing the initial, rapid binding of R6G. The dramatic effect of filtration on the initial anisotropy of the sols and freshly formed gels provides evidence for the presence of nanoparticles well after the gel point, which could also influence the long-term evolution of the monoliths. This point is discussed in more detail below.

Physical Properties of DGS/GLS Monoliths. To compare the rotational mobility of R6G molecules that are homogeneously distributed through the whole silica monolith to that of R6G molecules located exclusively in accessible channels and pores, the dye was incorporated at the sol stage (sample A) or allowed to diffuse through the preformed DGS/GLS monolith (sample B). Alternatively, a preformed DGS monolith was incubated first with GLS and then with R6G (sample C) to assess how the timing of GLS addition might influence the properties of the resulting DGS/GLS monoliths. For the studies of monoliths, all DGS sols were prepared by method A2 (i.e., by sonication in chilled water followed by filtration), and GLS levels were tested over the range of 5−20%.

Prior to anisotropy analysis, both the weight loss and shrinkage of samples A−C were tested to determine the overall time span required to reach a steady state and the effect of the preparation method on the ability of the material to resist shrinkage. The masses of both the DGS and DGS/GLS monoliths decreased gradually over a period of 35 days of aging and then leveled off (Figure 2a). The changes in mass were smallest for sample A, followed by samples B and C. This is consistent with the replacement of the nonvolatile glycerol with water during incubation to add either R6G or GLS. The higher proportion of water leads to a greater loss of mass as a result of solvent evaporation in

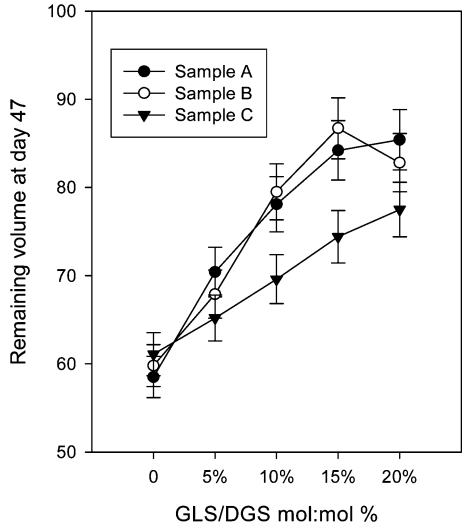

Figure 3. Shrinkage of DGS-derived monoliths containing various levels of GLS after 47 days of aging in air.

samples B and C. The overall loss of mass was also dependent on the amount of added GLS, decreasing as the amount of GLS increased (Figure 2b), consistent with the ability of the bound GLS to retain the entrapped water.[18]

To investigate the effects of preparation procedures on the physical structure of the resultant gels, shrinkage measurements were performed on DGS-derived monolithic gels containing various levels of GLS, as shown in Figure 3. In the absence of GLS, the samples shrunk to ∼60% of their initial volume, regardless of whether they were washed to remove the entrapped glycerol. Thus, entrapped glycerol does little to alter the overall shrinkage of materials. The shrinkage in volume decreased with increasing levels of GLS for all preparation routes. With increasing levels of GLS, samples A and B showed very similar extents of shrinkage, indicating the very similar matrix structures of samples for which GLS was added to the sol, regardless of whether washing was used to remove glycerol. In the case of sample C, however, much higher levels of GLS needed to be added to the monolith, relative to the amount added to the sol, to have the same effect on shrinkage. For example, retention of >80% of the volume was possible at GLS levels of 15 mol% for samples A and B, whereas monoliths formed by route C

containing as much as 20 mol% GLS retained only 75% of their volume. Materials formed by addition of GLS to a DGS sol also have much lower surface areas than pure DGS materials (33 m^2/g at 20 mol % GLS vs 591 m^2/g for DGS[18]), which is consistent with a much lower proportion of micropores. This likely contributes to the lower shrinkage obtained for such samples. Thus, the formation of GLS-coated nanoparticles appears to be important in ultimately minimizing shrinkage.

In cases where GLS was added to a preformed monolith, the material had a much higher surface area (195 m^2/g at 20 mol % GLS) relative to samples with a similar amount of GLS added to the sol. This is consistent with the presence of both micro- and mesopores,[18] indicating that GLS is likely unable to access micropores. These pores can thus produce high capillary stresses during drying, leading to shrinkage of the material. Overall, this shows that coating of particles prior to their incorporation into a network has a dramatic effect on silica morphology. However, it is also noted that addition of high levels of GLS to a preformed monolith can still lead to vastly reduced shrinkage, and thus modification of reactive silica surface sites with sugars still provides benefits in the production of low-shrinkage sol−gel-based materials.

SSFA Analysis of DGS/GLS Monolith Evolution. Based on the results of the mass-change and shrinkage studies, changes in anisotropy were monitored over a period of up to 60 days to follow the overall evolution of the monolith. Preliminary studies of the changes in R6G anisotropy within monolithic samples were done via steady-state anisotropy. More detailed analysis of these samples by TRFA is described in the next section. Anisotropy analysis of sol−gel-derived monoliths requires that the samples be optically transparent to avoid any scattering artifacts, which can significantly alter anisotropy values. Monoliths containing up to 20 mol % GLS exhibited excellent optical properties for SSFA and TRFA analysis. However, beyond this point, the monoliths were not optically transparent, possibly because of some flocculation of the GLS-coated nanoparticles prior to gelation. This process has been previously observed for GLS-coated Ludox[28] and further highlights the likelihood of there being GLS-coated nanoparticles in the DGS/GLS sol that cannot participate in network formation.

Given the significant amount of glycerol that is present inside the gel matrix (ca. 12% v/v), it is critical to understand the role of glycerol in controlling R6G anisotropy. For this reason, we prepared sample B as usual with a GLS level of 10%, but washed either with water containing 1 μM R6G at day 1 (24 h of incubation, identical to how sample B is normally processed) or with 1 μM R6G solutions containing 5% or 25% glycerol to retain a high level of glycerol in the washed samples. Note that these treatments will remove any excess free sugar from the matrix, so that the effect of glycerol can be more carefully examined. Inclusion of glycerol in the washing solutions led to a decrease in the anisotropy of R6G from 0.233 with 0% glycerol to 0.225 at 5% glycerol and 0.203 at 25% glycerol (samples aged 7 days). The observation of lower anisotropy values for samples containing glycerol is opposite to what would be

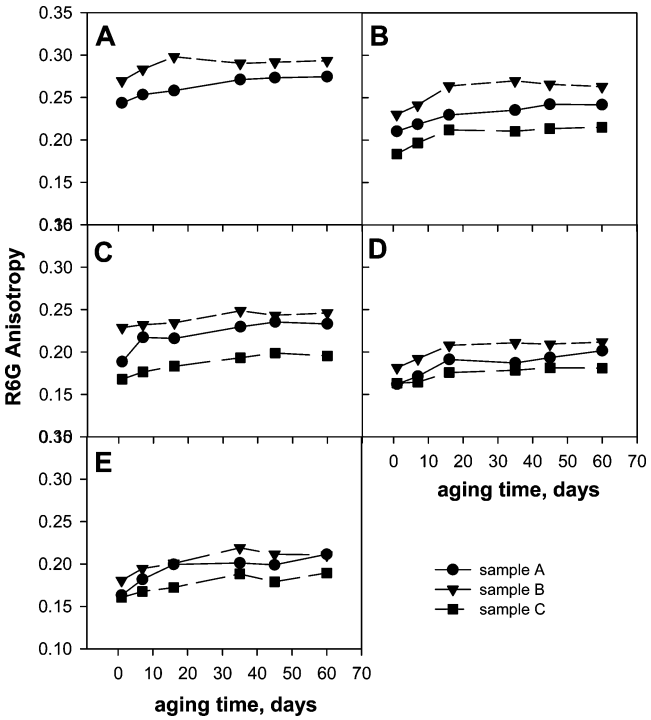

Figure 4. Steady-state anisotropy of R6G in DGS monoliths containing 0−20 mol % GLS. Experimental error, <0.6%; R6G concentration, 1 μM; excitation, 495 nm; emission, 551 nm. GLS concentration: (A) 0, (B) 5, (C) 10, (D) 15, and (E) 20 mol %. Monoliths were prepared (●, sample A) by mixing DGS, GLS, and R6G solutions at the sol stage; (▼, sample B) by equilibrating the preformed DGS/GLS monoliths with R6G solution; or (■, sample C)by subsequent equilibration of preformed DGS monoliths with GLS and R6G solutions, as described in the Experimental Section.

expected on the basis of microviscosity, clearly indicating that the effect is not related to changes in microviscosity. Rather, the presence of glycerol likely leads to a repartitioning of the R6G from the adsorbed to the free state, consistent with glycerol either solubilizing the probe or coating the silica surface and thus reducing the extent of R6G binding. It is also possible that the removal of glycerol when the samples are washed with water could result in nanoparticle aggregation and/or binding of particles to the monolithic silica, which would increase the SSFA of R6G, although TRFA data are needed to determine whether this is the case (see below). Overall, although glycerol has a relatively small effect, it does play a role in altering the anisotropy data.

Figure 4 shows the changes in steady-state anisotropy as a function of aging time for DGS/GLS gels containing different levels of GLS prepared by routes A−C. Consistent with the changes in mass noted above, there was a gradual increase in R6G anisotropy during the first 10−35 days of aging, after which the anisotropy essentially leveled off. This trend was consistently observed in all samples, independent of the GLS content. The observed increase in R6G anisotropy with aging likely reflects the drying process, which would result in repartitioning of the R6G from solution onto the surfaces of either nanoparticles or monolithic silica, and/or association of R6G-bound nanoparticles with the monolith, which would arrest nanoparticle rotation. It is not possible to distinguish between these scenarios on the basis of steady-state anisotropy data.

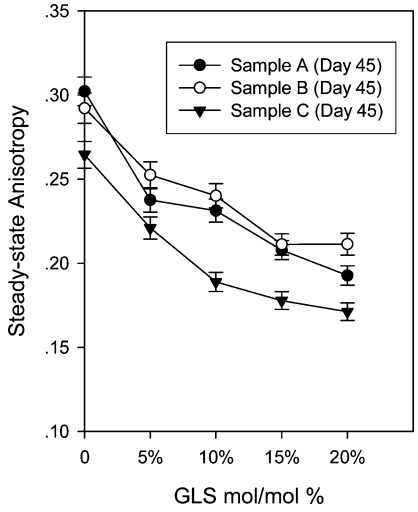

Figure 5. Steady-state anisotropy of R6G as a function of the level of GLS present in DGS-derived monoliths. Samples A−C were aged for 45 days prior to analysis. Experimental error is less than 0.6%.

Considering first the DGS samples without added GLS (Figure 4a), it is noted that materials derived by route A always exhibited a higher anisotropy than those derived by route B (consistent with the effect of glycerol, as noted above) and that neither sample approached the limiting anisotropy, $r_0 = 0.35$, obtained in the case where all of the motion of R6G is completely restricted in a fully formed monolithic silica matrix.[25] Overall, the SSFA data for the DGS samples show that, despite significant drying of the monoliths, R6G is still partially free to reorient within the sol−gel matrix. The low anisotropy values reflect the presence of R6G that is not rigidly bound to monolithic silica. However, as noted above, it is not possible to determine whether this fraction of R6G is located on the surface of rapidly rotating nanoparticles or is free in solution on the basis of the steady-state anisotropy data.

Addition of GLS to DGS materials generally led to a reduction in the steady-state anisotropy values, which tended to become lower as the concentration of GLS increased (Figure 5), indicating higher surface coverage at higher levels of GLS, as expected. The decreases in anisotropy appear to continue up to a GLS concentration of 20 mol %, beyond which flocculation was observed when GLS was added to the sol. However, even in cases where flocculation was not possible (sample C), these data tend toward an asymptote of 20 mol % GLS, suggesting that such a level can saturate the available silica surface in all samples. This is also consistent with the shrinkage values, which appear to plateau at 15−20 mol % GLS in all samples (see Figure 3).

As shown in Figure 5, the plateau anisotropy values reached after 45 days of aging were also dependent on the method used to form the material. In general, anisotropy was highest for samples formed by route B, followed by route A (because of the effect of glycerol), and finally route C. The lower anisotropy for sample C relative to sample B, both of which had glycerol removed by washing, indicates that addition of GLS to a preformed monolith results in an overall reduction in the fraction of immobile R6G molecules. This is consistent with a higher proportion of GLS being bound to the monolithic skeleton in sample C than in sample B, which would thus prevent rigid binding of R6G. On the other hand, GLS-modified sols (samples A and B) would be expected, on the basis of the SSFA data presented above, to have much of the GLS bound to silica nanoparticles. As a result, less GLS would be expected to be available to coat the monolithic skeleton, resulting in a higher proportion of R6G bound to the monolithic silica surface and hence a higher anisotropy for R6G within samples A and B. This situation is shown pictorially in Figure 6 and is supported by TRFA data presented below.

TRFA Analysis of DGS/GLS Monoliths. To gain further insight into the distribution of R6G among the monolith, nanoparticle surface, and free solution as a function of GLS concentration and preparation method, we employed TRFA to measure the proportion of R6G in each environment for the different samples. The TRFA parameters (ϕ_1, ϕ_2, f_1, f_2, and g) were interpreted using the model of rigid spheres.[30] According to this model, the R6G decay in the aqueous silica sol or sol−gel monolith is an overlap of three main

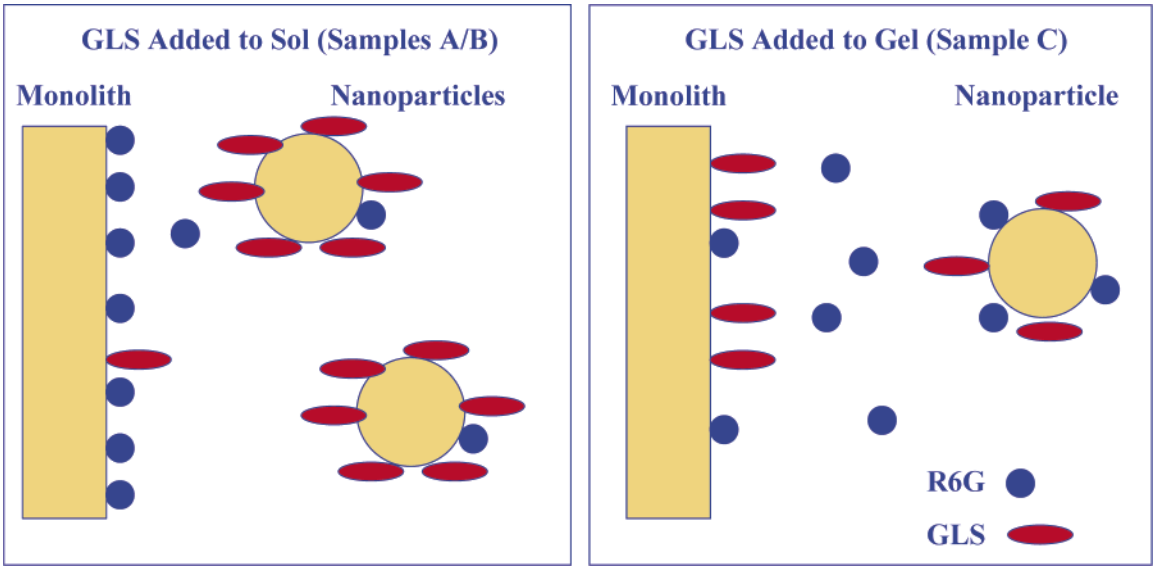

Figure 6. Schematic of the location of R6G and GLS in samples prepared by adding GLS to a DGS sol (samples A/B) or to a preformed DGS gel (sample C).

Table 1. TRFA Decay Parameters for R6G Entrapped in DGS Monoliths (Sample A) or Diffused in the Preformed DGS Monoliths (Sample B)[a,b]

sample	ϕ_1 (ns)	ϕ_2 (ns)	f_1	f_2	r_0	r	g	SS
				Sample A				
day 1	0.21	6.90	0.31	0.12	0.36	0.21	0.57	0.240
day 5	0.26	7.14	0.24	0.13	0.35	0.22	0.63	0.248
day 16	0.51	7.01	0.21	0.10	0.37	0.26	0.69	0.257
day 35	0.64	6.42	0.17	0.07	0.38	0.29	0.76	0.261
day 45	0.69	6.49	0.17	0.05	0.36	0.28	0.78	0.275
				Sample B				
day 1	0.20	6.73	0.32	0.12	0.37	0.21	0.56	0.240
day 5	0.29	6.29	0.17	0.10	0.34	0.25	0.73	0.269
day 16	0.51	6.02	0.14	0.05	0.35	0.28	0.81	0.281
day 35	0.59	5.78	0.11	0.03	0.38	0.33	0.86	0.287
day 45	0.63	5.91	0.11	0.02	0.37	0.32	0.87	0.284

[a] There is no sample C for this table, because GLS is absent in all gels. [b] All samples were tested in duplicate. ϕ_1, ±0.05 ns; ϕ_2, ±0.08 ns; f, ±0.01; r_0, ±0.01; fluorescence lifetime, 3.9 ± 0.01 ns; χ^2_R, 0.98−1.05. SS is steady-state anisotropy.

diffusional time components: (1) the picosecond rotational correlation time ϕ_1, attributed to the rotation of single R6G molecules dispersed in solvent-filled pores; (2) the nanosecond rotational correlation time ϕ_2, attributed to slower rotation of R6G molecules that are rigidly bound to small silica nanoparticles of radius $R < 2.5$ nm; and (3) the nondecaying anisotropy component, attributed to R6G molecules rigidly bound to the walls of the immobile silica network or to large particles of radius $R > 2.5$ nm whose rotational diffusion cannot be measured during the excited state of R6G ($\phi > 60$ ns).

As a starting point for TRFA analysis, DGS sols containing no GLS were prepared by routes A and B and subjected to TRFA analysis after various periods of aging. As reported in Table 1, all samples displayed a subnanosecond rotational component ($\phi_1 \approx 0.2-0.7$ ns), whose value increased with aging time owing to increases in local microviscosity as water evaporated, and a nanosecond rotational component ($\phi_2 = 6-7$ ns) whose value decreased slightly with aging time, possibly as a result of larger particles aggregating with the monolith, leaving only smaller particles free to rotate in the pores. Both samples initially showed significant fractions of both free ($f_1 = 0.31$) and immobile ($g = 0.57$) dye and a lower fraction of particle-bound dye ($f_2 = 0.12$). As aging proceeded, both samples showed a significant decrease in f_1, corresponding to a loss of free probe owing to adsorption as the solvent evaporated. There was also a significant decrease in f_2, which indicates that the proportion of rapidly rotating nanoparticles decreased with time, consistent with particle growth and/or association of particles with the monolithic silica network. A corresponding increase in the g value reflects an increasing amount of R6G that was rigidly bound and unable to rotate over a period of at least 60 ns, consistent with more dye being associated with the monolithic silica skeleton (either directly or owing to R6G-bound nanoparticles associating with the monolith) as aging proceeded. After 45 days, the samples showed 2−5% particle-bound R6G and 11−15% free dye. Thus, the low steady-state anisotropy values for samples A and B, relative to that obtained for R6G within sodium silicate derived materials,[25] is mainly related to a higher proportion of free dye, as most

Table 2. TRFA Decay Parameters for R6G Entrapped in DGS/GLS (10 mol %) Monoliths (Sample A), Diffused into Preformed DGS/GLS Monoliths (Sample B), and Diffused in DGS Monoliths Preequilibrated with GLS Solution (Sample C)[a,b]

	ϕ_1 (ns)	ϕ_2 (ns)	f_1	f_2	r_0	r	g	SS
				Sample A				
day 1	0.17	8.90	0.27	0.39	0.36	0.12	0.34	0.195
day 7	0.18	8.82	0.21	0.34	0.33	0.15	0.45	0.203
day 16	0.40	6.14	0.12	0.23	0.38	0.25	0.65	0.212
day 35	0.51	4.45	0.18	0.13	0.37	0.26	0.69	0.229
day 45	0.56	4.79	0.19	0.13	0.37	0.25	0.68	0.234
				Sample B				
day 1	0.20	6.89	0.21	0.37	0.34	0.14	0.42	0.213
day 7	0.21	7.22	0.07	0.17	0.35	0.27	0.76	0.224
day 16	0.40	6.05	0.05	0.16	0.38	0.30	0.79	0.237
day 35	0.42	5.89	0.11	0.08	0.36	0.29	0.81	0.245
day 45	0.36	5.76	0.10	0.07	0.36	0.30	0.83	0.251
				Sample C				
day 2	0.20	7.02	0.67	0.09	0.35	0.08	0.24	0.181
day 7	0.34	7.22	0.56	0.23	0.34	0.07	0.21	0.179
day 16	0.31	6.65	0.36	0.32	0.34	0.11	0.33	0.184
day 35	0.38	5.08	0.45	0.19	0.37	0.13	0.36	0.189
day 45	0.33	5.15	0.44	0.18	0.38	0.14	0.38	0.194

[a] Shortest aging time corresponds to the following: sample A, immediately after gelation; sample B, 1 day after gelation to allow for addition of R6G; sample C, 2 days after gelation to allow for addition of GLS and R6G. [b] All samples were tested in duplicate. ϕ_1, ±0.05 ns; ϕ_2, ±0.08 ns; f, ±0.01; r_0, ±0.01; fluorescence lifetime, 3.9 ± 0.01 ns; χ^2_R, 0.98−1.05 SS is steady-state anisotropy.

of the nanoparticles in the DGS-derived materials appear to be able to integrate into the network after this period of aging. The somewhat higher proportion of free dye and the lower g value in samples prepared by route A compared to those prepared by route B confirms that glycerol does lead to less overall binding of R6G to the silica surface, as a result of either blockage of silica sites or better solubility of the dye.

The TRFA data, in combination with the SSFA data, also provide insight into the DGS growth mechanism under the conditions used in this study (neutral pH, high silica concentration). Consistent with our previous study of DGS sols formed under such conditions,[26] primary particle formation occurs rapidly in the initial sol, and further growth occurs by aggregation of these particles to form larger secondary particles and ultimately a spanning network of particles (i.e., a gel). Further aging of the monolith results in continued aggregation of particles to form a denser, more mechanically stable monolith.

The effects of GLS are next considered, first focusing on the case where GLS is added to the sol and then moving to the case where GLS is added to a preformed monolith. As reported in Table 2, all samples derived by routes A and B exhibit both picosecond and nanosecond rotational correlation times and show the same general trend of an increase in ϕ_1 and a decrease in ϕ_2 as aging proceeds. However, compared to unmodified DGS materials, the GLS-modified monoliths initially displayed lower levels of free and immobile dye and a much higher fraction of dye associated with silica nanoparticles. This is consistent with a high proportion of nanoparticles that can bind R6G but are not able to associate with the monolithic skeleton. This is as expected, given that the SSFA data clearly show that GLS interacts with colloids present in the sol. The presence of GLS on the surface of free particles would be expected to result in an inability of

these particles to associate with the evolving gel network.

As aging proceeds, the value of f_2 drops steadily while the g value increases, consistent with either R6G repartitioning from particles to the monolith or R6G-bound particles associating with the monolithic silica skeleton. The f_1 value also tends to decrease somewhat with time, although this is more evident in samples that have had glycerol removed by washing. These data are consistent with slow partitioning of the dye to the silica surface as evaporation continues. By day 45, both samples A and B show relatively high g values (0.68−0.83), smaller f_2 values (0.07−0.13), and f_1 values in the range of 0.1−0.2. When compared to the comparable unmodified DGS samples, it is apparent that the addition of GLS (at a level of 10 mol %) does not lead to a significant increase in the fraction of free dye, but does cause a small decrease in the fraction of immobile dye and a small increase in the amount of particle-bound dye. In particular, for samples derived by route B, the presence of GLS ultimately does little to block the association of the dye with the monolithic silica surface (see Figure 6).

Samples prepared by route C displayed significantly different TRFA parameters than those prepared by routes A and B. Initially, samples derived by route C showed significantly less immobile dye ($g = 0.24$), a much higher amount of free dye ($f_1 = 0.67$), and a similar level of particle-bound dye ($f_2 = 0.09$) relative to unmodified DGS materials, consistent with GLS binding to the monolithic skeleton and preventing R6G adsorption. As aging proceeded, the level of free dye decreased while the amount of immobile dye increased, as expected on the basis of dye adsorption upon solvent evaporation. However, after 35 days, there was a significant decrease in the faction of rigidly bound dye ($g < 0.4$) and a markedly increased level of free dye ($f_1 > 0.4$) compared to either DGS or DGS/GLS materials formed by routes A or B. This further confirms that GLS is able to efficiently coat the preformed monolith. Unexpectedly, the GLS-coated materials formed by route C showed a significant increase in the proportion of R6G bound to silica nanoparticles as aging proceeded, again reaching a plateau after 35 days at $f_2 = 0.18$. The corresponding increases in f_2 and decreases in f_1 suggest that free dye preferentially associates with nanoparticles present in the pore solvent rather than with the monolithic silica, supporting the suggestion that the GLS preferentially coats the monolithic skeleton when added after gelation. The decrease in f_2 beyond day 16 is not fully understood, but it seems to correlate with increased levels of free dye, suggesting desorption of R6G. This might reflect continued modification of these nanoparticles with free GLS in the pore solvent.

Taken together, these data suggest that the time at which organosilane modifiers are added to a sol−gel-derived material is critically important to both the evolution and the ultimate properties of the resulting nanocomposite material. This therefore provides an additional control element beyond the rate of hydrolysis/condensation that is normally used to control modification by trialkoxysilanes. Addition of the modifier to the sol results in preferential coating of nanoparticles with the modifier, which then slowly associate with the evolving monolithic skeleton. On the other hand, addition of the modifier to a preformed monolith appears to result in preferential coating of the silica skeleton, resulting in a much lower degree of R6G−silica interactions and ultimately more free dye. Clearly, these effects need to be further evaluated using a larger number of modifiers and a wider range of times between monolith formation and addition of modifier. However, the results presented herein suggest that the time of addition of modifier can be used as a means to control the properties of organic−inorganic nanocomposite materials, including their ability to interact with entrapped dopants such as proteins or small molecules.

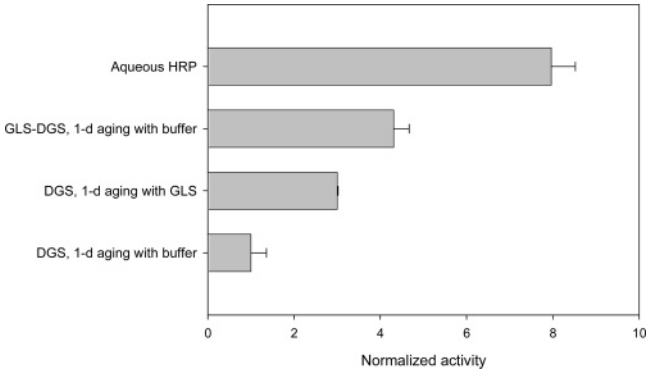

Figure 7. Activity of entrapped HRP in DGS monoliths with or without 10 mol % GLS added to the sol (GLS/DGS) or to a preformed DGS monolith. All samples contain 0.2 μg/mL HRP.

It should be noted that, although the data presented herein highlight the potential of TRFA for assessing the properties of monolithic sol−gel samples, the interpretation of the data relies heavily on the choice of model used to interpret the TRFA. On the basis of numerous past studies with particle-based silica systems, we chose to interpret our TRFA data using a hindered-rotor model and to interpret changes in the nanosecond decay time by assuming that nanoparticles are present in the monolith. Previous TRFA studies of sol−gel-derived materials have utilized different fitting models (e.g., two components, no hindered rotation) and interpreted the data on the basis of variable domains of differing microviscosity.[31−33] Although there is significant evidence to suggest that R6G binds strongly to silica surfaces and that the nanosecond component in R6G−silica systems is related to the presence of particles, it is clear that further studies using complementary methods will be needed to more fully evaluate the best model for interpreting both TRFA data and sol−gel growth processes.

Activity of Entrapped HRP in GLS-modified DGS. Figure 7 shows the effect of both the presence of GLS and the timing of GLS addition on the activity of HRP in gels that were aged for 1 day prior to testing. All data presented are for samples containing 10 mol % GLS; the activity values did not change significantly for levels of GLS ranging from 5 to 20 mol %, even though the data above suggest that 10 mol % of GLS is required to obtain full surface modification. Furthermore, the activity did not change appreciably for up to 7 days of aging for any samples (data not shown). The most noteworthy change in activity is related to the addition of GLS, which leads to a significant improvement in activity (3−4-fold) compared to that of unmodified DGS materials, regardless of when the GLS was added. The timing of

addition also had an affect on the activity compared to that of unmodified DGS, which increased from a 3-fold improvement when GLS was added to a preformed monolith to a 4-fold improvement when GLS was present in the DGS sol. Although the origin of this effect is not presently known, it is possible that GLS can act as an osmolyte to stabilize the protein during entrapment,[14] in addition to coating the silica surface prior to gelation, thus altering enzyme−silica interactions.[28]

At this stage, it is premature to speculate on the overall mechanism of the improved HRP activity when GLS is present in the sol. Previous work has shown that inclusion of GLS can alter porosity, protein accessibility, protein−silica interactions, and protein leaching.[17] Further work with additional enzymes, along with more detailed analyses of enzyme−silica interactions, enzyme accessibility, and leaching, will be required before this question can be answered. Studies on these issues will be reported in the future.

Conclusions

The steady-state and time-resolved fluorescence anisotropy of the probe rhodamine 6G entrapped in GLS-modified materials formed from DGS were measured as a function of time to examine the modification of the silica surface by the sugar. This measurement was based on the ability of the sugar to block electrostatic interactions between the cationic probe and the anionic silica surface. We note that, although there is a large body of work on the study of sol−gel materials by fluorescence methods, this is the first study that uses the nanoparticle metrology approach to study the surface properties of organically modified sol−gel materials. Indeed, this is the first work that describes the presence of silica nanoparticles within sol−gel monoliths, and it thus provides a new framework for modeling the evolution of sol−gel-based materials.

TRFA analysis suggests that addition of GLS to an evolving sol causes a high proportion of modified nanoparticles to be present that initially are not associated with the continuous polymer network. This is as expected, given that GLS can easily interact with colloids present in the sol.[28] The preferential presence of GLS on the surface of free particles results in inefficient coating of the monolithic material with GLS and, consequently, a high proportion of immobile dye associated with the monolith. The addition of GLS to a preformed monolith results in a significantly better coverage of the monolithic skeleton by GLS and also results in much higher levels of free dye than in systems where GLS is added to the sol. Entrapment of HRP into GLS-modified DGS materials showed that the presence of GLS was the most important factor affecting HRP activity, although the time of addition had some affect on activity, with optimal activity occurring when GLS was added to the sol. Thus, the modification of silica with hydrophilic sugar moieties provides a route to improve the performance of entrapped enzymes, in agreement with previous studies.[16,17]

Acknowledgment. We thank the Natural Sciences and Engineering Research Council of Canada; MDS-Sciex; the Ontario Ministry of Energy, Science and Technology; the Canadian Foundation for Innovation; and the Ontario Innovation Trust for financial support of this work. M.A.B. gratefully acknowledges the Canada Council for the Arts for a Killam Fellowship. J.D.B. holds the Canada Research Chair in Bioanalytical Chemistry.

CM051853Z